Convertible Perfect Absorber with Single Ring Resonator: Tunable Single Band/Dual-Band Visible

Pouria Zamzam[1] , Pejman Rezaei[2] ، Seyed Amin Khatami[3] and Zahra Mousavirazi[4]

Abstract: **This study proposes a single and dual-band tunable and convertible perfect absorber in the infrared band, consisting of a dielectric layer and a metallic bottom film. Primarily a tunable single-frequency absorber in the infrared region had been introduced. Subsequently, with the change in geometric structure, the proposed structure can be converted from infrared single-band to visible double-band frequency. The numerical simulation results indicate that the absorption spectrum of the single-band resonator is tuned from 337.4 THz to 210.2 THz, 227.3 THz, and 297.7 THz by changing effective parameters: ring width, ring height, and dielectric height. Next, by the parametric study of the proposed absorber dimensions, the absorption rate is obtained 99% more at the designed frequencies; lastly, the dual-band absorption with an average performance of 99.98% in the visible spectrum. The proposed plasmonic absorber in this research has a variety of applications, including sensing, imaging, wavelength-selective thermal emission, photodetectors, and so on.**

Index Terms— Metamaterial perfect absorber, Dual-band, Tunable, Infrared, Terahertz.

I. INTRODUCTION

Increasing bit rate and consequently the bandwidth, as the demand of today's telecommunications, motivates research towards higher frequencies, THz, infrared, and optics [1, 2]. Redesigning of well-known communications devices in microwaves, such as antennas [3-6], filters [7, 8], switches [9, 10], sensors [11-14], the antenna [15], etc, is a requirement of this process.

There is no doubt that any material that is not available in nature can be called metamaterial. Metamaterials are actually composite and artificial materials that have been engineered. They can also be described as materials that exhibit abnormal, unique, and peculiar properties. The first attempts at uncovering synthetic materials were made in 1898 by Jagadish Chandra Bose who researched materials with chiral properties. But one of the most important researches in this field dates back to 1968 when Veselago first presented a theoretical work on a material with a negative refractive index (NRI) with concurrent $\varepsilon, \mu < 0$.

Metamaterial perfect absorbers (MPAs) have recently been studied in microwaves, terahertz (THz), infrared and visible bands. Metamaterials, with the sub-wavelength, have attracted increasing attention because they have exhibited novel, unique and strange properties and are not found in nature at all such as negative permittivity, negative refractive index, cloaking behavior, invisibility, reverse doppler effects, and perfect absorption. Due to the significant benefits of full absorption, several studies have been reported on perfect absorbers and multi-layered MPAs after Landy. et al [16]. MPAs are usually realized by using lossy materials in periodic structures but in some periodic structures, materials are used without loss. The initial and basic mechanism of MPAs is that the incident electromagnetic wave fields are completely confined and gradually, inside these lossy materials, are consumed and become close to zero [17]. MPAs can be potentially used in many areas, such as plasmonic sensors, light-harvesting, thermal imaging, thermal emitter, and so on, while those with the narrowband are more desirable for single-pixel imaging and thermal measurement [18, 19].

There are usually two ways to achieve a multi-band perfect absorber. One is to Put several resonance structures next to each other and assemble with various geometric parameters in a coplanar such as the absorbers demonstrated by Huang et al [20] and Wang et al [21]. Another way is arranging the structures vertically and stacking, which is very effective in obtaining multi-band absorbers and it was applied in the absorbers presented by Mo et al. [22] and Grant et al. [23].

In the first model, the placement and assembling of the structure next to each other are called the unit cell of the absorber. One of its disadvantages is its extremely large size. The second model is faced with complexities and limitations in fabrication. It is known that classical (traditional) electromagnetic absorbers can be made based on a metal-dielectric-metal structure, which is made of a dielectric spacer sandwiched between two metals [24]. The first top layer is known as the resonator. This layer is primarily responsible for absorbing electromagnetic responses. In the paper [25], the electromagnetic force in the terahertz band generated by a cross-shaped absorber is introduced. Also in the paper [26, 27], ultra-wideband symmetric G-shape metamaterial-based microwave absorber, design and analysis of perfect metamaterial absorber in GHz and THz frequencies are introduced.

In [28], Quad-band polarization-insensitive metamaterial perfect absorber based on bilayer graphene metasurface is

1: Pouria Zamzam is the Electrical and Computer Engineering Faculty, Semnan University, Semnan, Iran
2: Pejman Rezaei is the Electrical and Computer Engineering Faculty, Semnan University, Semnan, Iran
3: Seyed Amin Khatami is Electrical and Computer Engineering Faculty, Semnan University, Semnan, Iran
4: Zahra Mousavirazi is 1604, 5720 cavendish Cote Saint Luc.
Corresponding author: zahra.mousavirazi@emt.inrs.ca

introduced. In [29, 30], ultra-thin dual-band polarization-insensitive and wide-angled perfect metamaterial absorber based on a single circular sector resonator structure and tunable metamaterial dual-band terahertz absorber are introduced, respectively. Also, Graphene-based terahertz metamaterial absorbers for broadband application are introduced in [31]. Absorber and sensor applications of complimentary H-shaped fishnet metamaterial for sub-terahertz frequency region are proposed in [32].

The dielectric spacer, which usually uses lossy material, is analyzed as a cavity. One of the reasons that the middle dielectric layer is chosen as a lossy material is because it increases the absorption width. The third and lowest layer in classic absorber structures is a thin metal film that ensures that the light wave is not completely transmitted from the structure. Due to the widespread use and large investments of optical communication instruments in the NIR frequency range $(760nm < \lambda < 2\mu m)$, this frequency range is very useful in telecommunications engineering. This paper demonstrates a new design concept for achieving a tunable single-band absorber with convertible capability to infrared region dual-band perfect absorber which consists of a single circular ring on the top of the dielectric layer and a thin metal film on the bottom.

The numerical results show that the absorption of the single band is more than 99% and the absorption spectrum is tuned from 337.4 THz to 210.2 THz, 227.3 THz, and 297.7 THz. The changes in effective parameters were then successively shown such as ring width, ring height, and dielectric height, and their effects on absorption peak and frequency displacement. The process was followed by achieving perfect dual-band absorption with an average of 99.98% by creating four gaps in the single resonator ring ***and changing the outer radius (r)*** in the visible region. Finally, for better apprehension, the absorption mechanism of the proposed structure and the electromagnetic field distribution is plotted and analyzed. The proposed electromagnetic absorber in this paper has potential application in spectral imaging, photodetector, energy harvesting, and so on.

II. Absorber Theory and Design

One of the main principles in designing an absorber is based on the theory of electromagnetic wave transmission and the mechanism of losses. Gradually, metamaterials can be described by complex permittivity $\varepsilon(\omega) = \varepsilon'(\omega) + j\,\varepsilon''(\omega)$ and complex permeability $\mu(w) = \mu'(w) + j\mu''(w)$, and the imaginary part of $\varepsilon''(w)$ and $\mu''(w)$ shows the EM losses. In the study of metamaterials, researchers often try to reduce imaginary parts to reduce losses. However, in the case of metamaterial absorbers, losses play a significant role. The resonance between the top metal layer and the bottom metallic film can be inferred from the absorption mechanism of the metamaterial absorber. Surface currents on the top layer caused by incident EM waves can induce electric resonance. Hence, the top metal layer can also interact with the bottom metallic film to form the magnetic dipole resonance. Our proposed absorber consists of a single circular metallic ring and metallic bottom film separated by a dielectric spacer, as shown in Fig. 1(a-c). The geometric parameters of the unit cell are shown in Fig. 1.

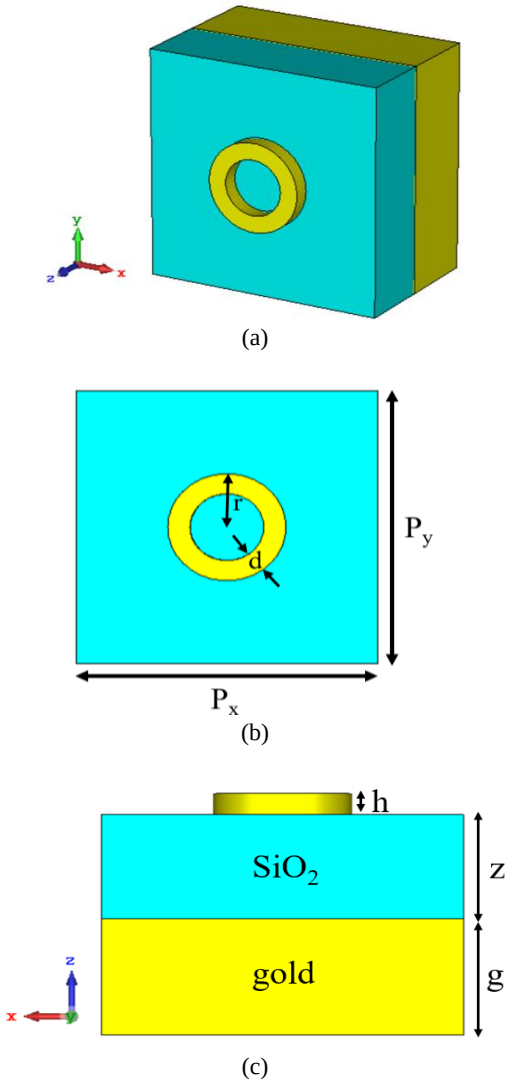

Fig. 1. The schematics of a single unit cell. (a) perspective view. (b) top view. (c) side view. The ring outer radius r=52 nm, d=20 nm, z=90 nm, g=100 nm, h=20 nm and $p_x = p_y = 286$ nm.

Based on the Finite Difference Time Domain (FDTD) method, the proposed absorber in this paper was calculated and optimized numerically. In all simulations, periodic boundary conditions were set in the x-and y-axis and a perfectly matched layer boundary condition was used along the z-axis. The dielectric layer is selected as SiO_2 substrate with a relative permittivity (ε =2.1+j0.0021) and two metallic layers on top and bottom made of gold by Drude model of $\varepsilon_{Au}=\varepsilon_\infty - \omega_p^2/\omega(\omega+j\mu)$ with plasma frequency $\omega_P=1.37\times10^{16}$ rad/s and collision frequency $\mu=4.07\times10^3$ rad/s and epsilon infinity is 9.5 [33, 34].

The absorptivity of the presented metamaterial absorber can be defined as A=1-T-R where T is transmissivity and R is reflectivity [35]. Because the thickness of the bottom Au film is much greater than the skin depth, the absorption can be obtained by A=1-R. Here it is assumed that the source is a plane wave that is normally incident onto the structure.

III. Result and Discussion

The unit-cell structure of the proposed design includes three functional layers: a ring resonator on the top, a dielectric spacer in the middle, and a bottom continuous metallic gold film. To study the efficiency of the proposed absorber, the model building and full-wave simulations were performed using the frequency domain solver in CST Microwave Studio.

Various parameters and the effect of their changes on peak absorption and frequency change had been investigated. The simulated absorption of the proposed absorber for different d values is shown in Fig. 2(a). Evidently, by decreasing the ring width by 2 nm, an increase in the absorption peak and a narrowing of the absorption band occurs, and then a perfect absorption with the absorptivity of more than 99.5% at 210 THz is obtained.

It is noteworthy mentioning that frequency change also occurs, but one of the advantages of checking multiple parameters separately is that it can be designed according to the desired frequency range and thus achieve a perfect narrow band absorber with a specific frequency.

Due to the constant value, d = 20 nm, the peak absorption is improved by a regular decrease of 10 nm from the dielectric thickness z respectively, while the other parameters are constant. As shown in Fig. 2(b), for z<40 nm; the peak absorption intensities are greater than 90% and the absorption is more than 98.8% when z=10 nm in 297 THz. Also, by adjusting the value of z, the frequency shifts and the absorption bandwidth can be further narrowed by reducing the thickness of the dielectric layer.

Also, the performance of the proposed absorber has been investigated by modifying ring height h from 20 nm to 6 nm, decreasing by 2 nm respectively when other parameters are constant (z=90, d=20), as shown in Fig. 2(c). The absorption peak intensities increase with decreased h. Then, with this decrease of ring height, the absorption band becomes narrower, which is desirable and the absorption is 99.5% at 227 THz.

Finally, the outer radius of the ring will be examined. Fig. 2(d), shows that by changing the outer radius (r) from 50 nm to 54 nm when the parameters of the structure are unchanged (d=6 nm, z=90 nm, and h=20 nm), the frequency changes from 218 THz to 206 THz. It should be noted that by changing this parameter, there is no change in the absorption peak and only allows it to have perfect absorption at the desired frequency by setting the above parameters.

Also, this structure is insensitive to changes in incident wave polarization in TE mode, which is an advantage for the proposed structure. As shown in figure 3(a), when the polarization angle increases from 0 to 45 degrees, there is a change of about 0.0001 in the absorption rate at this frequency and no frequency shifts are occurring. According to the symmetry of the structure, polarization angle from 0 to 45 degrees has been studied and we are sure that the results will be repeated from 45 to 90 degrees. Therefore, the proposed structure is insensitive to polarization angle. As shown in Figure 3(b) another advantage of the proposed structure, in addition to being perfect single-banded, and insensitive to incident wave polarization, has a wide incident angle.

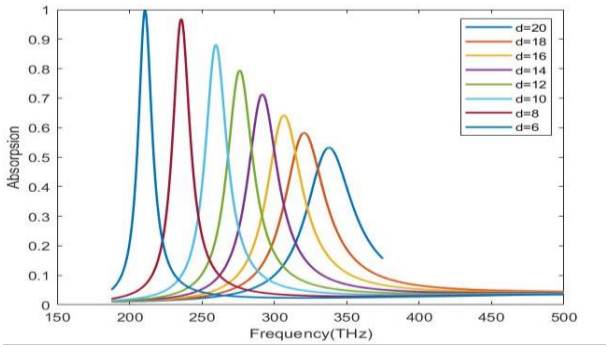

(a)

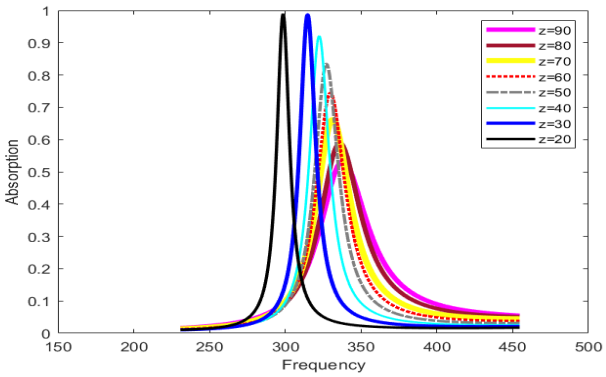

(b)

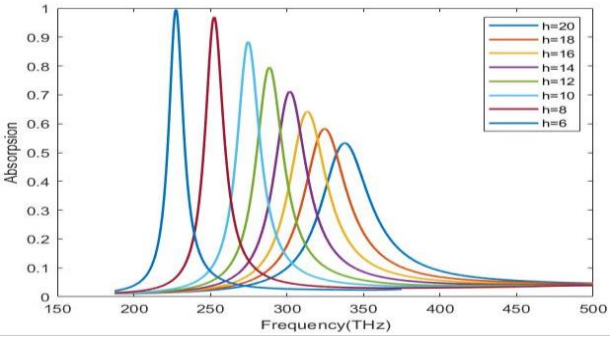

(c)

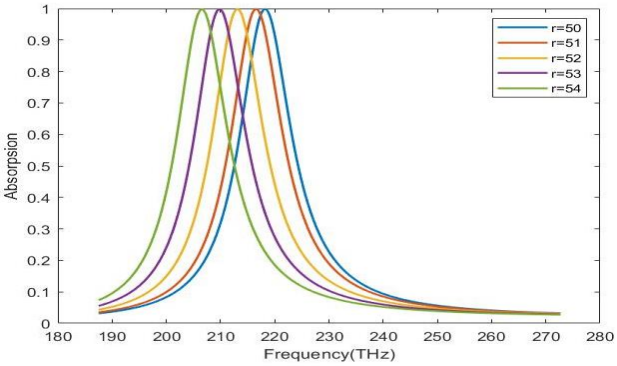

(d)

Fig. 2. The absorbance spectra of the proposed absorber for different geometric parameters: (a) Ring width "d". (b) dielectric thickness "z". (c) ring height "h". (d) outer radius "r".

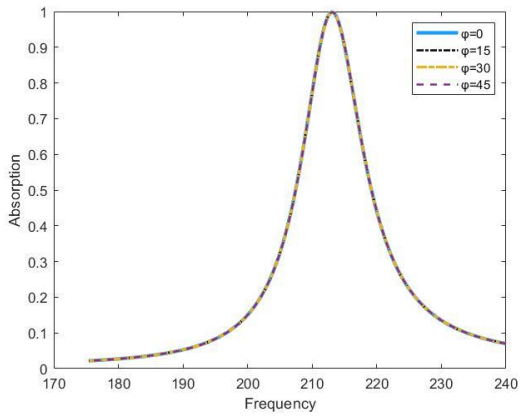

(a)

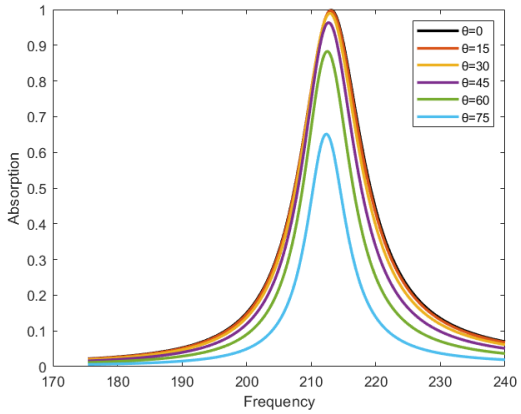

(b)

Fig. 3. (a) Dependence of the absorption spectra on the polarization angles of the normally incident wave. (b) Absorption spectra under different incidence angles with TE radiation.

To understand the physical mechanism underlying the absorption, we plotted the electric and magnetic field distribution in TM polarization for the resonant frequency. Note that accumulated surface charges can induce the magnetic field accountable for the magnetic resonance and resonance absorption.

The electric and magnetic resonance are overlapped at the resonant frequency and then the perfect absorption of the normal incidence is realized. As shown in Fig. 4(a) the electric field is mainly concentrated at both edges of the ring in the right and left sides of the ring resonator along the x-axis for the resonant frequency.

It is easy to find that the classic absorption mechanism is composed of an electrical resonance (realized by the top resonator layer) and a magnetic resonance (realized by the top and bottom metal layer), and it matches well with the results published in [6]. Note that the ring only excites the dipolar resonance. The accumulation of large surface charges causes the strong electric field distribution, and the existence of the strong electric resonance in the metallic array is due to the strong coupling of the metallic resonance structure, the dielectric spacer, and the bottom metallic film. For different resonance frequencies, the strong coupling appears in different parameters. As shown in Fig. 4(b) the magnetic field focuses on the surface of the ring along the y-axis.

As shown in Fig. 5, four gaps were used in the ring, while the other parameters remained constant. Then, by increasing the gap spacing, the effect of these gaps was investigated.

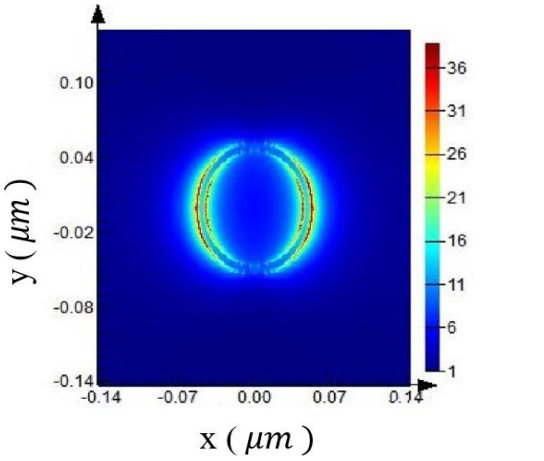

(a)

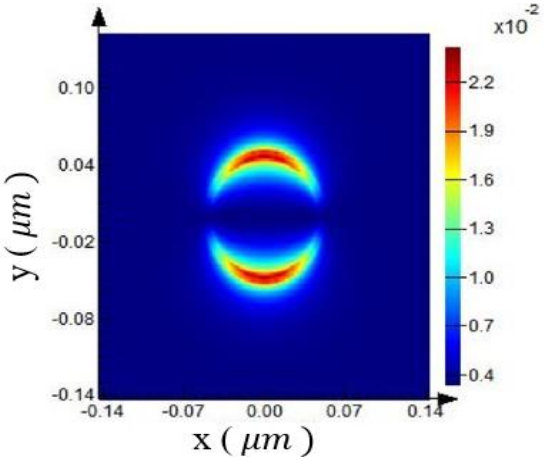

(b)

Fig. 4. (a) Electric field distribution in the interface between the top patterned metallic layer and the air layer for the proposed absorber at resonant frequency (TE mode). (b) Magnetic field distribution at resonant frequency (TE mode).

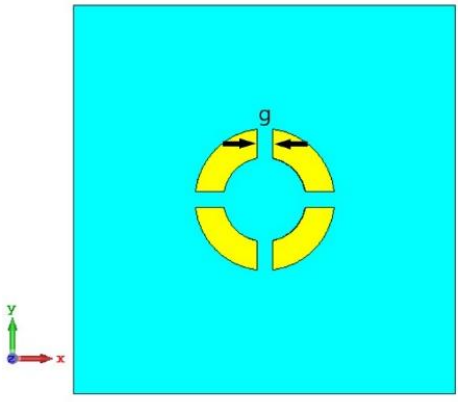

Fig.5. The schematics of a single unit cell with four gaps (top view).

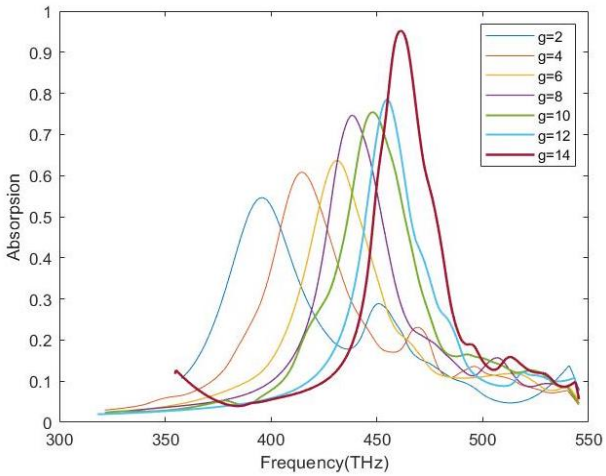

Fig. 6. The absorbance spectra of the proposed absorber with 4 gaps and with constant other parameters (d = 20 nm, h = 20 nm, z = 90 nm, r = 52 nm).

It can be seen in Fig. 6 by gradually increasing the gap spacing, the peak of absorption increases, and then 95% absorption is achieved at 461 THz.

Moreover, with a parametric study, we were able to obtain the structure of the dual-band using the same resonator ring. Using the same four gaps in the ring, a spacing of 2 nm (g = 2 nm), the value d = 6 nm, and with the change of the outer radius (r), finally, the average absorption is 99.7% at 446 THz and 470 THz, as shown in Fig. 7.

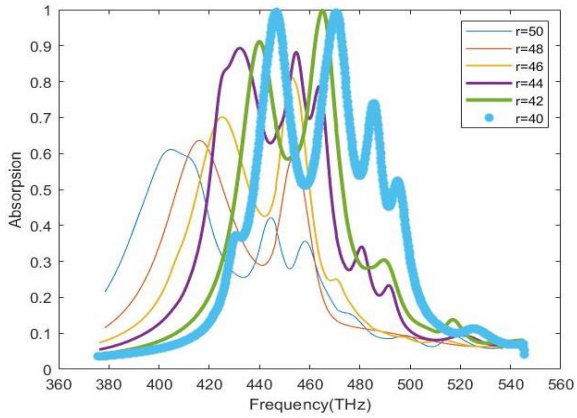

Fig.7. The absorbance spectra of the proposed absorber with gaps and with changes of outer radius (r).

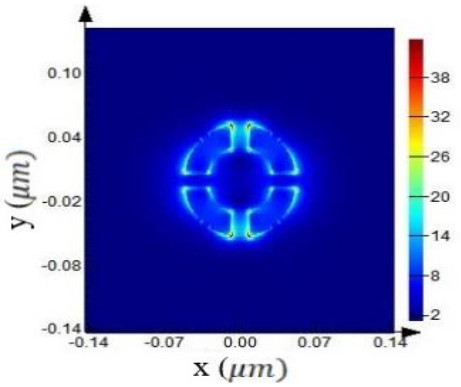

(a)

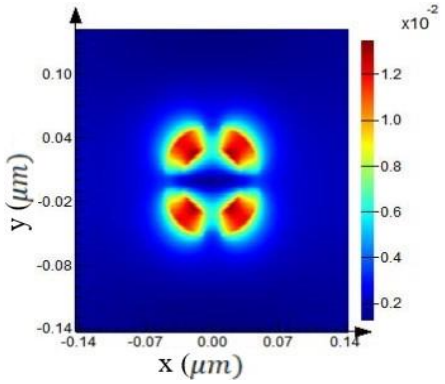

(b)

Fig. 8. (a) Electric field distribution of ring resonator with gaps at a resonant frequency. (b) Magnetic field distribution.

Also, as shown in Fig. 8(a) that the electric field concentrates near the cracks of gap rings along the y axis and unlike the electric field, there is a magnetic field on the four arms of this resonator, as you can see in Fig. 8(b). Finally, the compared performances of the proposed absorber and the previous works are collected in Table I.

TABLE I
They Compared Performances of the Proposed Absorber and the Previous Works

Ref.	Frequency (THz)	Cell dimension (μm)	Layers number	Absorptionrate
[31]	0.69	400 × 400	3	97.3%
[36]	4.24,5.89, 9.66, 10.62	3 × 3	3	97.74% Average
[37]	4.24, 6.86	9 × 9	3	97.18% Average
[38]	0.95	50 × 50	3	99.80%
[39]	1.6	50 × 50	2	95%
[40]	0.59	150 × 150	4	99%
[41]	1.26	150 × 150	3	99.93%
[42]	2.47-2.9	60 × 60	3	16% Bandwidth
Proposed	210.2 OR 227.3 OR 297.7 OR 337.4	0.286 × 0.286	3	99.98%

As shown in the table, the structure proposed in this paper has a perfect absorption peak, which is an advantage over other structures. Also as an important advantage, this structure in each of the frequencies 210.2, 227.3, 297.7, and 337.4 terahertz can provide perfect absorption depending on the different applications in these frequencies.

IV. Conclusions

In conclusion, we have illustrated a single-band absorber with convertible capability to dual-band absorber using single ring resonator based on metamaterial. The unit-cell structure of the design consists of a single circular ring on the top of the

dielectric spacer and the dielectric spacer on the continuous bottom metallic film. Results show with changed parameters in structure, absorption peaks with average absorptions higher than 99% can be gained. Finally, the circular ring was examined with 4 gaps and the effects of the spacing of these gaps. Then with a parametric study on the outer radius of the circular ring (r) with these gaps, a double-band absorber was obtained. Electric and magnetic field distributions are analyzed to understand the physical characteristics of the proposed metamaterial structure.

V. Acknowledgments

Also, the authors would like to thank the editor and reviewers for their constructive comments.

References

[1] Choi JH. (2015) High-speed devices and circuits with THz applications., CRC Press.

[2] Pereira MF, and Shulika O. (2011) Terahertz and Mid Infrared Radiation: Generation, Detection and Applications., Springer, Netherlands.

[3] Jafari Chashmi M., Rezaei P., and Kiani N. (2020) Y-shaped graphene-based antenna with switchable circular polarization., Optik, vol. 200, pp. 163321.

[4] Ullah S, Ruan C, Tanveer Ul Haq TUI and Zhang X. (2019) High performance THz patch antenna using photonic band gap and defected ground structure, J. Electromag. Wav. Appl., vol. 33, no. 15, pp. 1943-1954

[5] Jafari Chashmi M., Rezaei P., and Kiani N. (2020) Polarization controlling of multi resonant graphene-based microstrip antenna., Plasmonics, vol.15, no. 1, pp. 417-426.

[6] Jafari Chashmi M., Rezaei P., and Kiani N. (2019) Reconfigurable graphene-based V-shaped dipole antenna: From quasi-isotropic to directional radiation pattern., Optik, vol.184, pp. 421-427.

[7] Khani S., Danaie M., and Rezaei P. (2019) Size reduction of MIM surface plasmon based optical bandpass filters by the introduction of arrays of silver nano-rods., Phys. E: Low-dimens. Syst. Nanostruct., vol. 113, pp. 25-34.

[8] Khani S., Danaie M., and Rezaei P. (2019) Tunable single-mode bandpass filter based on metal-insulator-metal plasmonic coupled U-shaped cavities., IET Optoelec., vol. 13, no. 4, pp. 161-171.

[9] Khani S., Danaie M., and Rezaei P. (2020) All-optical plasmonic switches based on asymmetric directional couplers incorporating bragg gratings., Plasmonics, vol. 15, pp. 869-879.

[10] Khani S., Danaie M., and Rezaei P. (2020) Compact and low-power all-optical surface plasmon switches with isolated pump and data waveguides and a rectangular cavity containing nano-silver strips., Superlattices Microstruct., vol. 141, pp. 106481.

[11] Ghods MM., and Rezaei P. (2018) Graphene-based Fabry-Perot resonator for chemical sensing applications at mid-infrared frequencies. IEEE Photon. Technol. Lett., vol. 30, no. 22, pp. 1917-1920.

[12] Kiani S., Rezaei P., Fakhr M., An overview of interdigitated mic rowave resonance sensors for liquid samples permittivity detect o n, Ch. 7 in Interdigital Sensors, Springer, 2021. DOI: 10.1007/97 8-3-030-62684-6_7

[13] Sharma A.K., Kaur B. (2018) Analyzing the effect of graphene's chemical potential on the performance of a plasmonic sensor in infrared. Sol. State. Commun., Vol. 275, pp. 58-62.

[14] Nickpay M.R., Danaie M., Shahzadi A. (2021) Highly sensitive THz refractive index sensor based on folded split-ring metamaterial graphene resonators, Plasmonics. Doi:10.1007/s11468-021-01512-8.

[15] Nickpay M.R., Danaie M., Shahzadi A. (2019) Wideband Rectangular Double-Ring Nanoribbon Graphene-Based Antenna for Terahertz Communications. IETE J. Research, pp. 1-10.

[16] Landy NI., et al. (2008) Perfect Metamaterial Absorber. Phys. Rev. Lett., vol. 100, pp. 207402.

[17] Chen HT. (2012) Interference theory of metamaterial perfect absorbers., Opt. Express, vol. 20, pp. 7165-7172.

[18] Meng L., Zhao D., Ruan Z., Li Q., Yang Y., and Qiu M. (2014) Optimized grating as an ultra-narrow band absorber or plasmonic sensor., Opt. Lett., vol. 39, no. 5, pp. 1137-1140.

[19] He J., Ding P., Wang J., Fan C., and Liang E. (2015) Ultra-narrow band perfect absorbers based on plasmonic analog of electromagnetically induced absorption., Opt. Express, vol. 23, no. 5, pp. 6083-6091.

[20] Huang L., Chowdhury DR., Ramani S., Reiten MT., Luo SN., Taylor AJ., and Chen HT. (2012) Experimental demonstration of terahertz metamaterial absorbers with a broad and flat high absorption band., Opt. Lett., vol. 37, no. 2, pp. 154-156.

[21] Wang DG., Liu HM., Hu WX., Kong HL., Cheng LL., and Chen QZ., (2013) Broadband and ultra-thin terahertz metamaterial absorber based on multi-circular patches., Eur. Phys. J. B, vol. 86, no.7, pp. 1-9.

[22] Wen QY., et al. (2013) A polarization-independent and ultra-broadband terahertz metamaterial absorber studied based on circular-truncated cone structure. Acta. Phys. Sin-CH. ED., vol. 62, pp. 237801.

[23] Grant J., Ma Y., Saha S., Khalid A., and Cumming DRS. (2011) Polarization insensitive, broadband terahertz metamaterial absorber., Opt. Lett., vol. 36, no.17, pp. 3476-3478.

[24] Fu J., et al. (2015) The electromagnetic force in the terahertz band generated by a cross-shaped absorber., Sol. State. Commun., vol. 204, pp. 5-8.

[25] Ghods MM., and Rezaei P. (2017) Ultra-wideband microwave absorber based on uncharged graphene layers, Electromagnetic waves and applications., J. Electromag. Wav. Appl., vol. 32, no. 15, pp. 1950-1960 (2017).

[26] Naqavi SA., Baqir MA. (2018) ultra-wideband symmetric G-shape metamaterial based microwave absorber., J. Electromag. Wav. Appl., vol. 32, no. 16, pp. 1492976.

[27] Dincer F., Karaaslan M., and Sabah C. (2015) design and analysis of perfect metamaterial absorber in GHz and THz frequencies., J. Electromag. Wav. Appl., vol. 29. no.18, pp. 1043030.

[28] Zamzam P., Rezaei P., Khatami SA. (2021) Quad-band polarization-insensitive metamaterial perfect absorber based on bilayer graphene metasurface., Phys. E, vol. 128, pp. 114621.

[29] Lou C.Y., et al. (2015) tunable metamaterial dual-band terahertz absorber., Sol. State. Commun., Vol. 222, pp. 32-36.

[30] Ahmadi H., et al. (2021) Graphene-based terahertz metamaterial absorber for broadband application., Sol. State. Commun., vol. 323, pp. 114023.

[31] Aksimsek S. (2020) design of an ultra-thin, multiband, micro-slot based terahertz metamaterial absorber., J. Electromag. Wav. Appl., vol. 34, no. 16, pp.1809532.

[32] Faruk A., and Sabah C. (2018) Absorber and sensor applications of complimentary H-shaped fishnet metamaterial for sub-terahertz frequency region., Optik, vol. 177, pp. 64-70.
[33] Ordal MA., Long LL., Bell RJ., Bell SE., Bell RR., Alexander RW., and Ward CA. (1983) Optical properties of the metals al, co, cu, au, fe, pb, ni, pd, pt, ag, ti, and w in the infrared and far infrared., Appl. Opt., vol. 22, pp. 1099-1119.
[34] Norouzi Razani AH., Rezaei P. (2022) Broadband polarization insensitive and tunable terahertz metamaterial perfect absorber based on the graphene disk and square ribbon, Micro Nanostruct., vol. 163, 107153.
[35] Wang BX., Wang GZ., Wang LL., and Zhai X. (2015) Design of a five-band terahertz absorber based on three nested split-ring resonators., IEEE Photon. Technol. Lett., vol. 28, no. 3, pp. 307-310.
[36] Norouzi Razani A, Rezaei P. (2022) Multiband polarization insensitive and tunable terahertz metamaterial perfect absorber based on the heterogeneous structure of graphene., Opt. Quant. Electron., vol. 54, 407.
[37] Zamzam P., Rezaei P. (2021) A terahertz dual-band metamaterial perfect absorber based on metal-dielectric-metal multi-layer columns., Optic. Quant. Electron., vol. 53, pp. 109.
[38] Zheng W., Li W., and Chang SJ. (2015) A thermally tunable terahertz metamaterial absorber., Optoelec. Lett., vol. 11, pp. 18-21.
[39] Liu J., Fan L., Ku J., and Moe L. (2016) Absorber: a novel terahertz sensor in the application of substance identification., Opt. Quant. Electron., vol. 48, no. 2, pp. 80.
[40] Kong H., Li G., Jin Z., Ma G., Zhang Z., and Zhung C. (2012) Polarization-independent metamaterial absorber for terahertz frequency., J. Infrared, Millimeter, and Terahertz Wav., vol. 33, pp. 649-656.
[41] Ling X., Xhiao Z., and Zheng X. (2018) Tunable terahertz metamaterial absorber and the sensing application., J. Mater. Sci. Mater. in Electron., vol. 29, pp. 1497-1503.
[42] Nickpay M.R., Danaie M., Shahzadi A. (2021) A wideband and polarization-insensitive graphene-based metamaterial absorber., Superlatt. Microstru. vol. 150, pp. 106786.